ELSEVIER

Journal of Hydrology 235 (2000) 88–103

Journal of Hydrology

www.elsevier.com/locate/jhydrol

Groundwater mixing dynamics at a Canadian Shield mine

M. Douglas[a,1], I.D. Clark[a,*], K. Raven[b,2], D. Bottomley[c,3]

[a]*Department of Earth Sciences, Ottawa-Carleton Geoscience Centre, University of Ottawa, 140 Louis Pasteur, P.O. Box 450, Stn. A, Ottawa, Ont., Canada K1N 6N5*

[b]*Duke Engineering and Services, 265 Carling Avenue, Suite 208, Ottawa, Ont., Canada K1S 2E1*

[c]*Atomic Energy Control Board, Waste and Decommissioning Division, 280 Slater St., Ottawa, Ont., Canada K1P 5S9*

Received 16 August 1999; revised 24 March 2000; accepted 11 May 2000

Abstract

Temporal and spatial variations in geochemistry and isotopes in mine inflows at the Con Mine, Yellowknife, are studied to access the impact of underground openings on deep groundwater flow in the Canadian Shield. Periodic sampling of inflow at 20 sites from 700 to 1615 m depth showed that salinities range from 1.4 to 290 g/l, with tritium detected at all depths. Three mixing end-members are identified: (1) Ca(Na)–Cl Shield brine; (2) glacial meltwater recharged at the margin of the retreating Laurentide ice sheet at ~10 ka; and (3) modern meteoric water. Mixing fractions, calculated for inflows on five mine levels, illustrate the infiltration of modern water along specific fault planes. Tritium data for the modern component are corrected for mixing with brine and glacial waters and interpreted with an exponential-piston flow model. Results indicate that the mean transit time from surface to 1300 m depth is about 23 years in the early period after drift construction in 1979, but decreases to about 17 years in the past decade. The persistence of glacial meltwater in the subsurface to the present time, and the rapid circulation of modern meteoric water since the start of mining activities underline the importance of gradient, in addition to permeability, as a control on deep groundwater flow in the Canadian Shield.

Keywords: Groundwater; Canadian Shield; Mixing; Environmental isotopes; Geochemistry; Brine; Tritium; Con Mine; Radioactive waste

1. Introduction

Consideration of deep crystalline rocks for the burial of high-level radioactive waste has generated an interest in deep groundwater circulation in Shield settings. Of concern is the rapid advective transport of contaminants to the surface through discontinuities in the rock mass. Considerable research has been carried out examining groundwater flow in fractured rock, including in situ testing in underground openings. However, little work has been done to glean safety-relevant hydrogeological data from the various gold and base metal mines that exist in crystalline settings of the Canadian Shield, despite similarities to the proposed setting of a radioactive waste repository. Their depths generally reach or exceed the 500–1000 m depth proposed for a repository, and the time the Shield mines are operational is often close to the 50-year time frame proposed for operation of a radioactive waste repository.

In this study, we examine the impact of underground openings on hydrogeologic conditions at the

* Corresponding author. Tel.: +1-613-562-5773; fax: +1-613-562-5192.

E-mail address: idclark@uottawa.ca (I.D. Clark).

[1] Present address: Applied Petroleum Technologies, 1200 East Hackberry, Suite C, McAllen, TX 78501, USA. Tel.: +1-956-664-0371.

[2] Tel.: +1-613-232-2525.

[3] Tel.: +1-613-996-0366.

0022-1694/00/$ - see front matter
PII: S0022-1694(00)00265-1

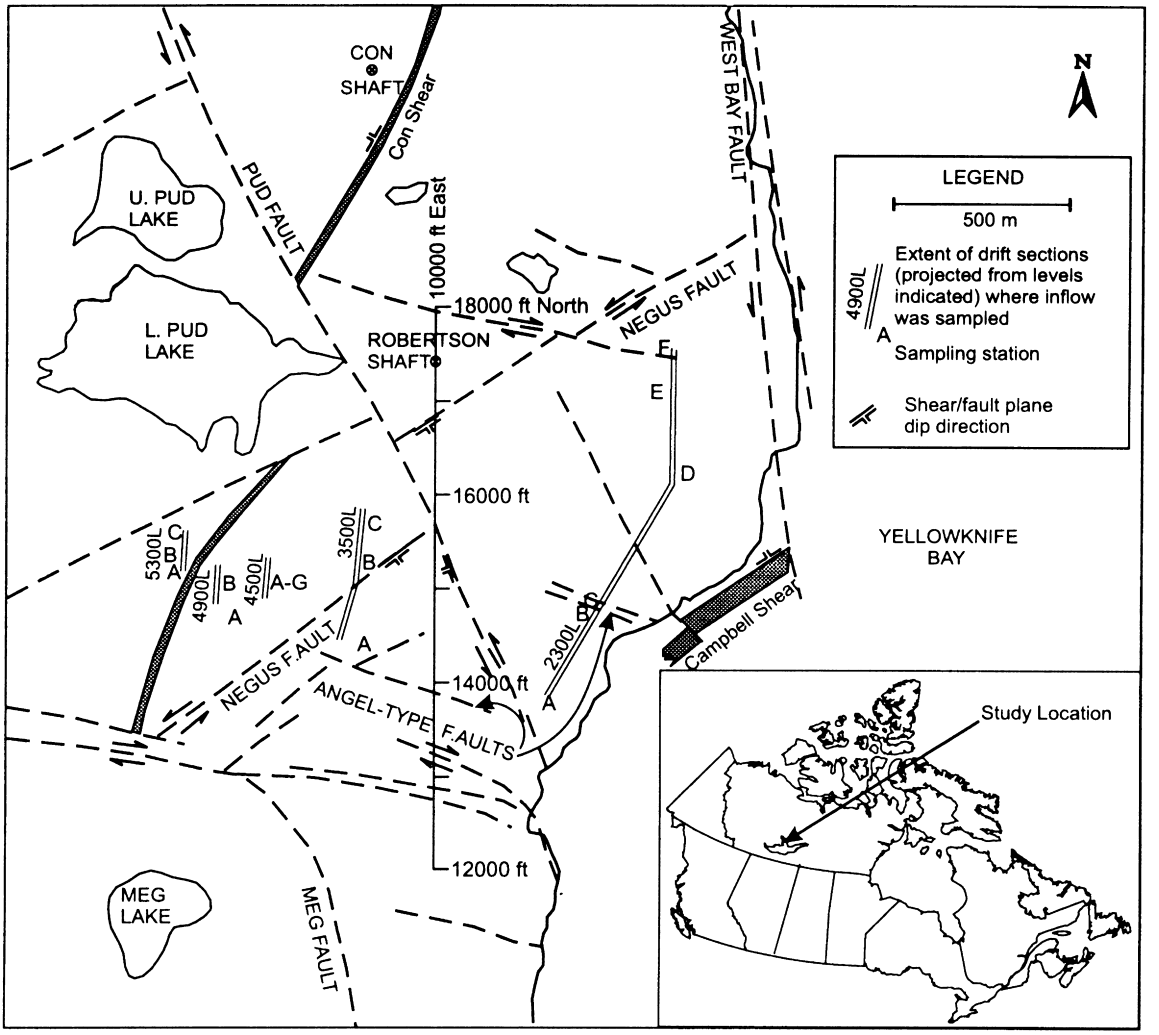

Fig. 1. Map of the southern area of the Con Mine showing mineralized shear zones, faults, and surface water bodies in the area sample. The drift sections represent the north–south limits between regular sampling locations at each level, and illustrate the westerly offset of drifts with increasing depth.

Con Mine in Yellowknife, N.W.T., Canada (Fig. 1). This mine, in operation since 1937, is presented as a physical analogue for the hydrogeological perturbations that could be caused by the construction and operation of a repository for high-level nuclear waste. Construction of an underground repository can be expected to disturb the regional groundwater flow system, controlled by discontinuities (faults and joints) in the rock mass, by creating steep hydraulic gradients between surface and depth and inducing flow towards excavated areas. Following closure of the repository, the discontinuities would represent transport pathways for radionuclides, as regional flow systems are re-established. Although a repository site in a faulted Archean greenstone setting may not be considered, the Con Mine nonetheless represents an extreme case that provides insights into the rates of groundwater circulation and mixing in crystalline rock.

The objectives of this study are to determine the extent to which modern meteoric water may be migrating into mine excavations and to trace

Table 1
Con Mine sample locations—physical data

Samplesite	Depth (m)	Level	Northing	Borehole number	Borehole drill date	Fault(s) intersected	Flow rate (l/min)current
23-A	701	2300	14 140	seep		?	2
23-B	701	2300	15 053	Y-5	Jan-1970	Angel	<0.5
23-C	701	2300	15 053	Y-6	Dec-1969	Angel	<0.2
23-D	701	2300	16 673	B-654	Apr-1958	B-101 shear	0.01
23-E	701	2300	16 848	B-646	Apr-1958	Negus	2
23-F	701	2300	17 300	B-660	May-1958	Negus	<3
35-A	1067	3500	14 700	B-9362	Apr-1995	?	20
35-B	1067	3500	15 386	B-8906	Apr-1995	Angel	4
35-C	1067	3500	15 410	seep		Angel	
35-D	1067	3500	15 800	B-9452	Sep-1995	Negus	<2
39-A	1189	3900	17 060	seep		?	
43-A	1311	4300	21 098	B-1912	June-1970	Westbay	
43-B	1311	4300	25 500	B-134	Apr-1981	?	
43-C	1311	4300	26 200	seep			
45-A	1372	4500	15 000	B-5316	Sep-1987	Pud/neg	2
45-B	1372	4500	15 110	B-3357	Mar-1980	Negus	5
45-C	1372	4500	15 110	B-3618	Feb-1981	Negus	0.5
45-D	1372	4500	15 115	B-3450	Feb-1980	Negus	10
45-E	1372	4500	15 200	B-5318	Sep-1987	Ang/neg	max 45;(1-2 in 1994)
45-F	1372	4500	15 286	B-3316	n/a	Pud/angel	
45-G	1372	4500	15 360	B-3362	Dec-1979	Angel	1
49-A	1494	4900	14 905	B-5310	Sep-1987	Pud	1
49-B	1494	4900	15 130	seep		Angel	
53-A	1615	5300	15 100	B-7126	Mar-1991	Angel	2
53-B	1615	5300	15 395	B-5586	Jun-1988	Pud	0.3
53-C	1615	5300	15 400	B-6709	Jul-1990	Angel	0.5

groundwater flow pathways and transit time from surface to depth. The study approach is based on a characterization of groundwaters using geochemistry and environmental isotopes. Notable in Shield settings is the occurrence of brines at depth, with a characteristic Ca–Cl chemistry and enriched ^{2}H contents, which contrast with recent meteoric infiltration. This provided a basis to distinguish between groundwater types and to establish flow pathways and mixing relationships. A third end-member identified during this study is a groundwater characterized by low $\delta^{18}O$ and $\delta^{2}H$ values, originating from the infiltration of glacial meltwaters during the early Holocene deglaciation. Temporal and spatial changes in these mixing relationships, corroborated by tritium measurements, provided insights to rates of groundwater circulation.

1.1. Geological setting

The Con Mine is located on the southern outskirts of the town of Yellowknife, on the west side of Yellowknife Bay, an arm of Great Slave Lake (Fig. 1). Surface relief is less than 75 m in the district, which has an elevation of about 200 m above sea level. There is considerable exposure of bedrock, and in lower-lying areas there is thin drift cover, with occasional lakes. The mine is situated in volcanics of the Yellowknife Greenstone Belt, in the southwestern part of the Slave province of the Canadian Shield. The earliest structural displacements within the volcanic sequence are mineralized shears formed during the emplacement of the granodiorite batholith of the Western Plutonic Complex (McDonald et al., 1993), two of which, the Campbell and the Con, are targets for gold exploration.

Late Precambrian activity produced steeply dipping faults in three main orientations (Lindberg, 1987; Henderson and Brown, 1996). The oldest is illustrated by the Negus Fault (NE–SW) having left-lateral horizontal displacement (Fig. 1). The Pud Fault (NNW–SSE) is the best example of the second fault trend on

which the horizontal (left-lateral) movement is dominant. It is younger than the NE–SW faulting as shown by a 290 m horizontal offset of the Negus by the Pud at the mine. Probable splays from this fault are visible in the mine. Passing immediately to the east of the mine is the West Bay Fault, a major regional feature, having left-lateral displacement of 5 km (Campbell, 1948). Its orientation is closer to N–S than the Pud fault in the area of the mine. The third set of faults, having an E–W trend, are collectively referred to as the Angel-type faults, with similar orientations and permeabilities. They show right-lateral movement along vertical planes, and most probably are the same age as the NNW oriented Pud fault.

During the Phanerozoic, the region around Great Slave Lake experienced inundation during the relatively widespread Late Ordovician to Devonian marine incursion. Strata include marine evaporites like those currently found at Gypsum Point southwest of Yellowknife. The district experienced extensive Quaternary glaciation, and was covered by the Laurentide ice sheet up to approximately 10 ka (Dyke and Dredge, 1989), after which glacial Lake McConnell extended eastward over the area until ca 9 ka (Craig, 1965).

1.2. Mine hydrology

Mine workings cover an area of approximately 3.5 by 1.5 km, with N–S drifts progressively offset westwards with depth down the westerly dipping and mineralized Campbell shear zone. The south end of the mine was studied, covering an area of approximately $1.5 \times 1.5\ km^2$ extending from surface to the 5300 level at 1.6 km depth, thus providing a three-dimensional array of subsurface sampling locations. This area of the mine has seen virtually no ore extraction, and so only the drifts and boreholes have contributed to the disturbance of the hydrogeological flow conditions. Drifting at the 2300 level was completed within 10 years of initial shaft emplacement, to 750 m below surface in 1946. Another shaft was driven to 1890 m in 1974 allowing drifting to proceed at the lowest levels. The 4500 level was opened in 1979, providing a 17 year monitoring record, and the 5300 level was extended in 1990. The metric depths are given in Table 1 although we use mine designations in feet to specify drift levels.

Exploration boreholes have been drilled on all levels in fan arrays along the drifts. Borehole lengths average 175 m. Most that produced water were drilled within 15° of horizontal, and had intersected at least one of the steeply dipping faults. Boreholes drilled on the 2300 and 3500 levels flowed at rates of up to 90 l/min indicating that the Negus and Angel-type faults are important conduits for groundwater flow. The Angel-type faults have the highest measured hydraulic transmissivities (up to $2 \times 10^{-2}\ m^2/s$), whereas the NW–SE Pud fault has the lowest (up to $4 \times 10^{-4}\ m^2/s$) (Intera Consultants Ltd, 1997). This is consistent with stress analysis results from the mine which indicate major principal stress directions varying from E–W at the 3500 level, sub-parallel to the Angel fault orientation, to WSW–ENE by the 5700 level, sub-parallel to the Negus Fault. Pud-orientated faults are normal to the major principal stresses. The faults described here are associated with all of the inflow observed down to the 5300 level.

2. Sampling and analytical procedures

Sampling stations were established for all underground sites with sufficient flow. Samples have been identified with a number–letter–number code such that the first two digits represent the drift level, and the letter indicates position in the sequence from south to north. The final number represents one of four sampling excursions made to observe temporal variability (1: May-1995; 2: July-1995; 3: Nov-1995; 4: Jun-1996). For example, 23–A–4 is the most southerly station on the 2300 level, sampled in June 1996 (Table 1).

Flowing boreholes were fitted with packer and valve installations, and a flow cell then used to monitor groundwater pH, Eh, electrical conductivity, dissolved oxygen, and temperature before exposure to air. Alkalinity titrations were performed at surface at the end of the day's underground shift. Major cations were analysed by ICP-AES at the Geological Survey of Canada. Anions were analysed by HPLC (Dionex) at the University of Ottawa. Samples were filtered at 0.45 μm, and a split was acidified with HNO_3 for cation analysis.

Oxygen-18 in water was analysed on a triple collector VG SIRA 12 mass spectrometer. Analytical

Table 2
Geochemical composition of Con Mine groundwaters. Concentrations in ppm. Saturation index (SI calculated as log (IAP/KT)

Sample	Date	pH	T°C	Ca^{2+}	Na^{+}	Mg^{2+}	K^{+}	Cl^{-}	SO_4^{2-}	HCO_3^{-}	TDS	SL_{cal}	SI_{gyp}
23-A-4	Jun-1996	6.40	–	612	1130	27.0	10.5	2180	1050	27.5	5050	−1.8	−0.1
23-B-4	Jun-1996	6.94	11.2	616	699	57.4	12.4	1560	1130	273	4360	0.1	−0.2
23-C-4	Jun-1996	7.06	11.1	541	374	49.2	11.1	762	1110	356	3200	0.4	0.0
23-D-4	Jun-1996	5.95	–	6080	8430	339	51.8	25 700	9	9.8	40 800	−1.8	−1.9
23-E-4	Jun-1996	7.19	12.1	215	100	60.6	10.4	142	483	390	1500	0.3	−0.6
23-F-4	Jun-1996	7.19	11.0	215	146	59.8	10.8	199	491	388	1510	0.2	−0.7
35-A-4	Jun-1996	7.60	17.6	1670	2000	32.8	14.2	6390	581	24.4	10 800	0.1	−0.2
35-B-4	Jun-1996	7.28	17.2	226	245	32.8	8.8	610	154	442	1720	0.5	−1.1
35-D-4	Jun-1996	7.02	17.6	925	872	73.3	12.2	3180	603	127	5830	0.1	−0.2
45-A-4	Jun-1996	7.09	24.0	4800	3680	76.6	25.5	15 100	584	31.7	24 000	0.0	−0.1
45-B	Jul-1980	6.60	23.0	12900	10900	268	111	37 100	746	28.0	62 400	−0.2	−0.1
45-B	Apr-1981	–	–	10500	8050	209	53.1	29 400	715	34.0	49 300	–	–
45-B	Jun-1985	7.25	24.0	4220	2970	73.0	22.3	18 000	723	34.5	26 200	0.3	−0.2
45-B-4	Jun-1996	7.31	22.0	2520	2480	42.6	17.3	7850	609	31.7	13 600	0.1	−1.0
45-D	Jul-1980	6.35	23.0	15700	9420	250	110	31 900	198	69.0	58 000	+0.0	−0.6
45-D	Jun-1985	6.95	24.0	14300	6970	162	62.3	38 600	214	108	60 700	0.8	−0.5
45-D-4	Jun-1996	6.31	22.0	14500	7200	145	55.4	41 300	738	51.2	64 300	−0.2	−0.0
45-E-4	Jun-1996	6.35	22.0	19000	9250	159	69.6	57 900	465	47.0	87 300	−0.2	−0.1
45-F-4	Jun-1996	–	–	48500	21700	257	170	14 1000	489	–	213 000	–	–
45-G	Jul-1980	6.25	22.5	54400	35800	1340	483	13 5000	–	–	228 000	–	–
45-G	Apr-1981	–	–	23400	13600	468	109	60 200	715	48.0	99 200	–	–
45-G-4	Jun-1996	6.36	22.0	38200	17300	231	133	90 200	369	26.8	147 000	−0.4	−0.1
49-A-4	Jun-1996	7.20	23.3	27100	14800	248	100	78 000	642	7.3	121 000	−0.1	0.1
49-B-4	Jun-1996	6.50	–	53400	23100	195	191	139 000	443	15.0	217 000	−0.3	0.3
53-A-4	Jun-1996	6.64	26.0	62800	25700	188	230	186 000	247	12.0	276 000	0.3	0.3
53-B-4	Jun-1996	–	–	68800	28300	232	255	160 000	229	11.6	259 000	–	–
53-C-4	Jun-1996	6.50	25.0	73500	29800	287	272	185 000	130	14.6	290 000	0.2	0.0

precision (2σ) was 0.10‰. Results are expressed relative to Vienna Standard Mean Ocean Water (VSMOW). Corrections for the effect of high salinities were made using the method of Sofer and Gat (1972). Deuterium was analysed on hydrogen obtained by reduction of water on zinc. Samples were first injected onto a stainless steel filter in an evacuated, heated inlet, which vapourized the sample and removed solutes. Water vapour was frozen onto the zinc in a glass breakseal cooled with liquid nitrogen, then reduced to H_2 at 450°C for analysis on a double collector VG 602E mass spectrometer. Results are normalized to VSMOW, with a 2σ precision of 1.5‰. Sulphate was precipitated as $BaSO_4$ by addition of excess $BaCl_2 \cdot 2H_2O$. The barite was converted to SO_2 by combustion with copper oxide and quartz at 1100°C. $\delta^{34}S$ was analysed on a triple collector VG SIRA 12 mass spectrometer. Precision (2σ) is 0.20‰. Results are expressed relative to the Cañon Diablo Troilite (CDT) standard. Oxygen-18 in sulphate was analysed at the Environmental Isotope Laboratory, University of Waterloo. CO_2 was produced by combustion of sample with graphite in molybdenum foil, with oxidation of co-produced CO completed in a high voltage chamber. Method precision (2σ) is 0.5‰. Results are expressed relative to VSMOW. Dissolved inorganic carbon (DIC) in water samples was converted to CO_2 by reaction with phosphoric acid. $\delta^{13}C$ was analysed on a triple collector VG SIRA 12 mass spectrometer. Precision (2σ) was 0.10‰. Results are expressed relative to the Vienna Pee Dee Belemnite (VPDB) carbon standard. Carbon-14 was determined by accelerator mass spectrometry at the Isotrace Laboratory, University of Toronto. Tritium was analysed at the Environmental Isotope Laboratory, University of Waterloo by liquid scintillation counting following electrolytic enrichment, with a detection limit of 0.8 TU (1 TU = 1 ^{3}H per 10^{18} ^{1}H).

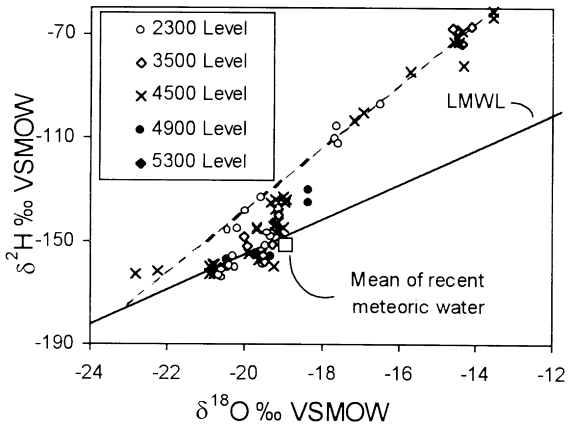

Fig. 2. $\delta^{18}O$ vs. $\delta^{2}H$ in precipitation and groundwater. The local meteoric water line (LMWL) is from data collected between 1989 and 1993 (Moorman et al., 1996) and has a relationship of $\delta^{2}H = 6.75\ \delta^{18}O - 20.1‰$.

3. Results and discussion

3.1. Groundwater salinity

Major ion results are presented in Table 2 for the final sampling excursion in June 1996. Salinity follows a general logarithmic increase with depth, although local variations of over an order of magnitude difference can occur within a single drift where water is associated with different faults. Groundwater contained Cl^- concentrations ranging between 48 ppm and 194 g/l and maximum salinity of approximately 290 g/l.

The saline waters brines are Ca–Na:Cl type, recognized elsewhere at depth in the Canadian Shield (Frape et al., 1984; Macdonald, 1986). Thermodynamic calculations using SOLMINEQ88 (Kharaka et al., 1988, Table 2) show that the brines are close to saturation with respect to gypsum. Earlier investigations at Yellowknife and other locations across the Canadian Shield give brine salinities of up to 325 g/l TDS (Frape and Fritz, 1982; Frape et al., 1984;

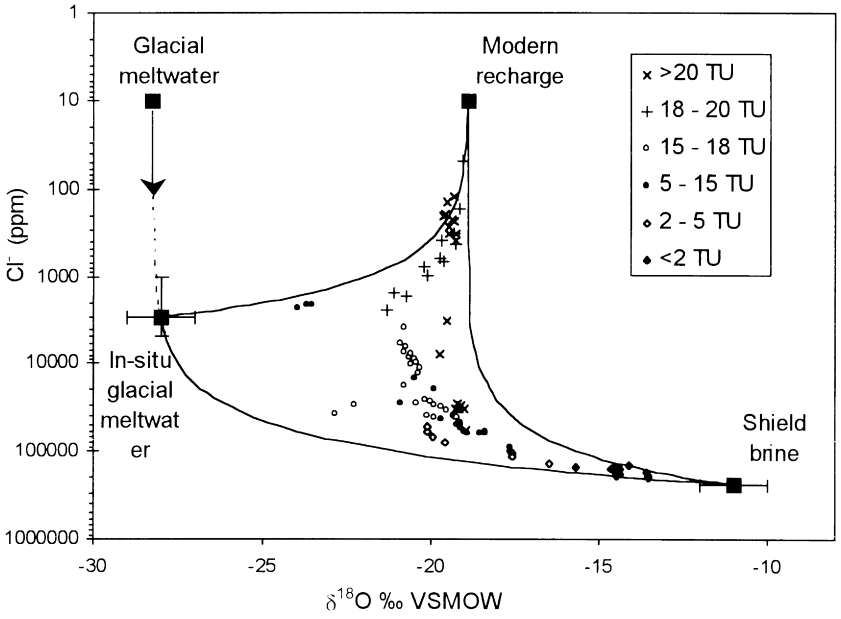

Fig. 3. Relationship between $\delta^{18}O$ and chloride concentration in groundwaters, with mixing lines plotted between end-members. Glacial meltwater is the direct infiltration from the base of the overlying ice sheet margin at ca 10 ka. The in-situ meltwater end-member is presumed to have derived minor Cl^- through leaching from the rock mass during subsurface residence over the Holocene period. The ±1‰ $\delta^{18}O$ error bars are shown for both the in-situ glacial and the brine mixing end-members. The Cl^--axis error bars represent ±2000 ppm for the in-situ glacial water, and ±20 000 ppm for the brine.

Bottomley et al., 1994; Gascoyne and Kamineni, 1994).

Shallow groundwaters have salinity levels that are generally less than 10 g/l, with either a Na–Ca:Cl–SO_4, or Ca–Na:SO_4–HCO_3–Cl geochemical facies. These groundwaters are saturated with respect to calcite, which can be observed as euhedral crystals in fractures. Gypsum is close to saturation in most groundwaters, and is oversaturated in the deepest brines. The origins of the high sulphate concentrations are determined on the basis of their isotopic composition, discussed below.

3.2. Origin of mixing components—^{18}O, ^{2}H and Cl^-

The isotopic composition of groundwater is shown in Fig. 2, with the local meteoric water line for Yellowknife. The $\delta^{18}O$ composition of the low salinity ($Cl^- < 1000$ ppm), high ^{3}H waters from the shallowest (2300) mine level is −20‰. A trend of ^{2}H enrichment to values above the LMWL is observed for deep, high salinity groundwaters. This ^{2}H enrichment is characteristic of Shield brines where the isotopic composition of brine end-member is attributed to extensive alteration of the original isotopic composition of the water through mineral hydration and water–rock interaction (Fritz and Reardon, 1979; Frape and Fritz, 1982). The strong variation in salinity along this enrichment trend is due to variable mixing of brine with modern meteoric waters (Frape and Fritz, 1982).

A second trend of ^{18}O and ^{2}H depletion towards more negative values exists for shallow and intermediate depth groundwaters. Examination of salinity (Cl^-) with $\delta^{18}O$ reveals a third mixing component that is depleted in ^{18}O. This is attributed to mixing with a glacial meltwater end-member recharged along the margin of the Laurentide Ice Sheet at the end of the past glaciation (Clark et al., 2000), and which has been observed elsewhere in Shield settings (Bottomley et al., 1990).

The three-component mixture in mine groundwaters is more clearly observed in a plot of $\delta^{18}O$ against Cl^- (Fig. 3). Groundwaters do not fall on a simple mixing line between Shield brine and modern meteoric waters, but are shifted to lower $\delta^{18}O$ values due to the component of glacial meltwater. In this diagram, the mixing end-members are defined as:

1. Recent meteoric water, corrected for mixing with glacial melt water in the subsurface, has $\delta^{18}O \sim -18.9$‰ and low salinity ($Cl^- < 10$ ppm). This $\delta^{18}O$ value has been determined from the low salinity groundwaters by linear extrapolation to $Cl^- = 0$ ppm (Clark et al., 2000). This component is also, for most samples, tritium-bearing (i.e. modern).
2. The Canadian Shield brine has high salinity ($Cl^- = 240$ g/l) with $\delta^{18}O = -10$‰ and no measurable tritium. These values are based on a comparison of the most saline waters in this study with calculations for a rock-equilibrated brine at NaCl saturation (Frape and Fritz, 1982; Pearson, 1987).
3. In-situ glacial end-member with a $\delta^{18}O$ value of −28‰, no tritium, and a Cl^- salinity of up to about 4000 ppm. The $\delta^{18}O$ value is derived from other studies for the $\delta^{18}O$ value of the Laurentide Ice Sheet (Hillaire-Marcel et al., 1979; Dansgaard et al., 1982) and includes a correction for up to 15% contemporary precipitation on the ice sheet margin. Considering that the early Holocene climate in the Arctic was approximately 6°C warmer than present (Cwynar and Ritchie, 1980; Koerner and Fisher, 1990) precipitation at that time would be up to 3‰ enriched over the mean for modern precipitation. The minor salinity in the glacial end-member is apparent from the data in Fig. 3, which include no ^{18}O-depleted, low-Cl^- values. This salinity is attributed to leaching of residual salinity from low permeability microfractures within the host bedrock during the ~10 ka subsurface residence time.

3.3. Mixing calculations

The composition of individual samples can be expressed in percentage of the three end-members. The component fractions are determined by the following series of equations, where the subscripts T, B, G and R represent total, brine, glacial and recent waters. The total of all fractions must obey the volumetric mass balance equation:

$$C_T = C_B + C_G + C_R \quad (1)$$

Table 3
Isotope and mixing data for Con Mine groundwaters

Sample	Date	$\delta^{18}O$	$\delta^{2}H$	^{3}H (TU)	Cl^- (ppm)	Mixing fractions		
						Recent	Brine	Glacial
23-A-4	Jun-9	−23.7	−187	11.9	2177	0.48	0.00	0.52
23-B-2	Jul-9	−20.7	−167	19.6	1692	0.79	0.00	0.21
23-C-3	Nov-9	−20.1	−162	19.6	971	0.87	0.00	0.13
23-D-4	Jun-9	−20.2	−146	< 0.8	25 731	0.66	0.10	0.24
23-E-2	Jul-9	−19.5	−152	26	263	0.94	0.00	0.06
23-E-3	Nov-9	−19.5	−158	23.9	322	0.93	0.00	0.07
23-F-4	Jun-9	−19.6	−157	–	199	0.92	0.00	0.08
35-A-4	Jun-9	−20.7	−161	17.9	6389	0.75	0.02	0.22
35-B-3	Nov-9	−19.7	−155	21	391	0.91	0.00	0.09
35-D-3	Nov-9	−19.7	−156	24.6	7680	0.85	0.03	0.12
39-A-4	Jun-9	−19.1	−140	–	53 700	0.54	0.22	0.24
45-A-2	Jul-9	−19.1	−139	10.7	47 045	0.60	0.19	0.21
45-B	Jul-8	−22.8	−163	3	37 100	0.28	0.14	0.57
45-B	Apr-8	−22.3	−162	34	29 400	0.41	0.11	0.48
45-B	Jun-8	−20.8	−159	57	18 000	0.65	0.07	0.28
45-B-2	Jul-9	−20.6	−165	18.7	10 201	0.74	0.04	0.22
45-B-3	Nov-9	−20.4	−160	14.2	12 967	0.74	0.05	0.21
45-B-4	Jun-9	−20.6	−162	15.1	7845	0.76	0.03	0.21
45-D	Jul-9	−19.7	−145	47	31 900	0.66	0.13	0.21
45-D	Jun-8	−19.3	−135	45	38 590	0.64	0.16	0.20
45-D-4	Jun-9	−19.2	−144	17.2	41 271	0.63	0.17	0.20
45-E-2	Jul-9	−19.1	−143	21.2	33 130	0.71	0.13	0.16
45-G	Jul-8	−14.3	−82	3	135 000	0.39	0.56	0.04
45-G	Apr-8	−19.0	−133	44	60 200	0.50	0.25	0.25
45-G-2	Jul-8	−18.4	−135	11.8	63 650	0.54	0.26	0.20
45-G-3	Nov-9	−18.5	−135	13.3	63 766	0.52	0.26	0.22
45-G-4	Jun-9	−17.6	−115	8.8	90 166	0.41	0.37	0.22
49-A-4	Jun-9	−19.6	−134	4.4	77 986	0.30	0.32	0.38
49-B-4	Jun-9	−16.5	−97	2.4	139 149	0.13	0.57	0.30
53-A-3	Nov-9	−14.4	−74	< 0.8	183 368	0.00	0.76	0.24
53-A-4	Jun-9	−14.5	−73	0.9	185 555	−0.03	0.77	0.26
53-B-4	Jun-9	−14.4	−69	1	159 890	0.19	0.66	0.15
53-C-4	Jun-9	−13.5	−62	1.4	185 215	0.07	0.77	0.16
53-D-4	Jun-9	−15.7	−84	–	152 589	0.11	0.63	0.26

where $C_T = 1$ and the three remaining components are unknown values. These components can be determined using an isotope mass balance equation and a Cl^- mass balance equation:

$$C_T\delta^{18}O_T = C_B\delta^{18}O_B + C_G\delta^{18}O_G + C_R\delta^{18}O_R \quad (2)$$

$$C_TCl_T^- = C_BCl_B^- + C_GCl_G^- + C_RCl_R^- \quad (3)$$

By substitution in Eq. (2) for C_R from Eq. (1), and rearrangement, we obtain:

$$C_B = \frac{C_T(\delta^{18}O_T - \delta^{18}O_R) + C_G(\delta^{18}O_R - \delta^{18}O_G)}{\delta^{18}O_B - \delta^{18}O_R} \quad (4)$$

and substitution in Eq. (3) for C_B from Eq. (1) to obtain:

$$C_R = \frac{C_T(Cl_T - Cl_B) - C_G(Cl_G - Cl_B)}{Cl_R - Cl_B} \quad (5)$$

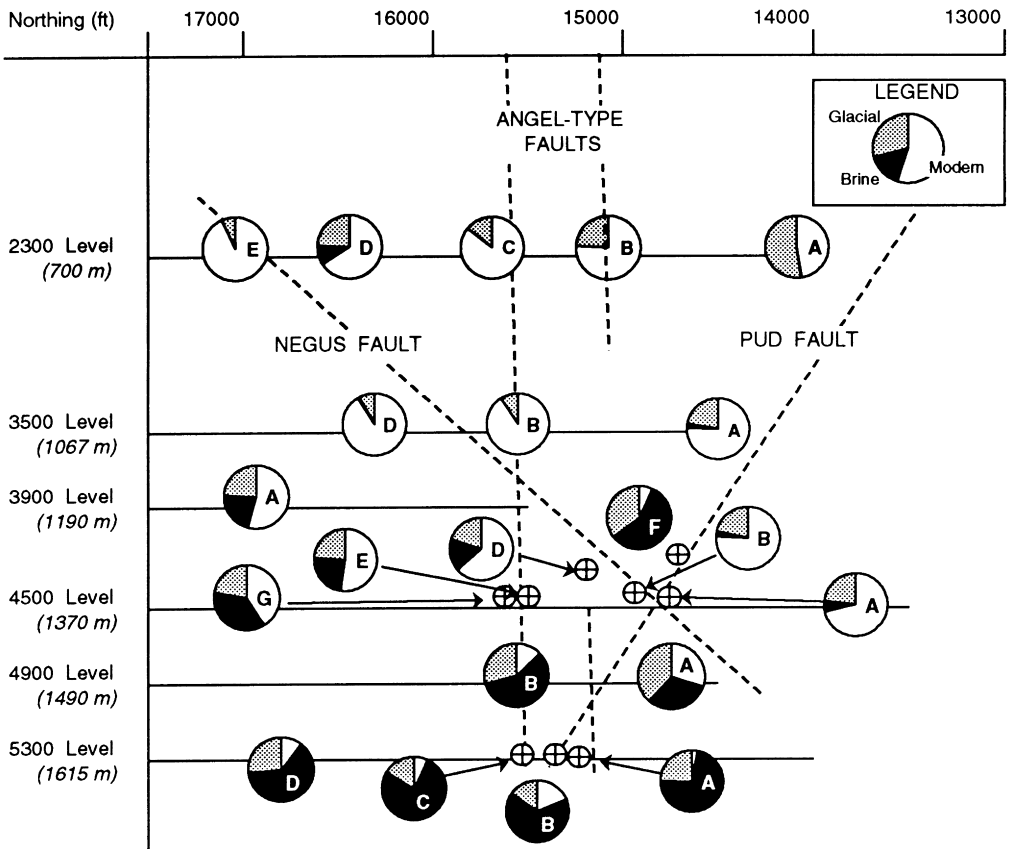

Fig. 4. Spatial distribution of end-member components in groundwaters, for most recent sample in study (Table 3). Vertical section along 10 000 ft. East mine grid line (Fig. 1), with mine levels and faults projected to section. Modern groundwater contributions show that the Negus and Angel-type faults are important conduits for groundwater flow whereas the Pud fault, oriented normal to regional stress, has the lowest rates of modern inflow.

There is a unique solution for C_G when $C_T = 1$. The other two components are calculated by back-substitution. Results of these calculations have been made for representative data for each sample site (Table 3), and are presented as pie diagrams related to drift level and borehole location in Fig. 4.

Samples from the 4500 level were used to evaluate the error in the mixing calculation imparted by uncertainties in the $\delta^{18}O$ and Cl^- values selected for the glacial and brine mixing end-members. The values selected for the modern meteoric water are well constrained and so are not evaluated here. However, data trends in Fig. 3 suggest that the Cl^- content of the in-situ glacial meltwater may vary along the meltwater—brine mixing line between about 2000 and 4000 ppm. Higher concentrations than this would leave a number of lower salinity samples outside of the mixing envelope. The mixing ratios were found to be most sensitive to variations in $\delta^{18}O$ of the glacial or brine end-member, although in both cases, the effect of the change in the modern component on tritium modelling was minor. Using sample 45-B as an example, the effect is observed to be greatest for the early (July 1980) data, which has a larger component of glacial water than later samples from this site. The effect of decreasing the $\delta^{18}O$ value for the glacial water end-member by 1‰ changes the component of modern water from 27 to 32%. For a 1‰ error in the $\delta^{18}O$ value of the brine end-member, the modern component is affected by less than 2%. For later data, which has a larger component of modern meteoric water, the error is less than 3% for a 1‰ difference

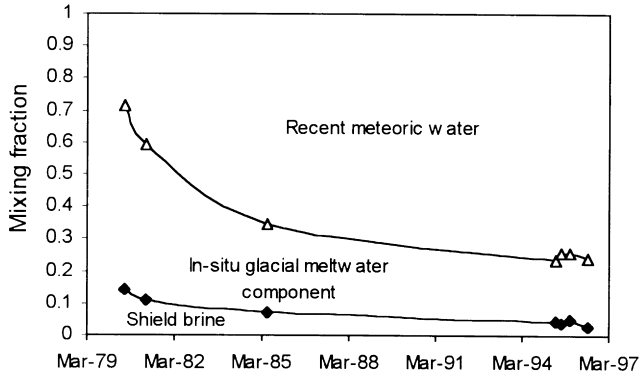

Fig. 5. Relative changes in mixing fractions of groundwater from 45-B between July 1980 and June 1996. Drift construction took place in 1979, and the borehole was drilled in March 1980. Dashed curves extrapolated to March 1980, with 0% modern groundwater.

in the value of the glacial water end-member, and less than 1% for a 1‰ error in the brine $\delta^{18}O$ value. These errors are within the limits of uncertainty in the tritium modelling, discussed below.

3.4. Spatial and temporal distribution of water types in the mine

Representing inflows according to their relative composition of the three water types provides an interesting perspective on the spatial and temporal distribution of modern, glacial and brine waters in this setting. From Fig. 4 we observe a high proportion of recent meteoric waters in the upper mine levels, and dominantly brines at depth. This is consistent with a temporal trend towards increased meteoric water in the discharge (Fig. 5) due to depressurization around the mine openings and the creation of steep downward gradients. Glacial meltwaters are presented at all levels, representing over 50% of inflow at some sites. Distribution is related to the relative permeability of faults. The highly permeable Negus fault has channeled a high proportion of recent meteoric water to the 3500, 4500, and 5300 levels. However, distinctly different water compositions within this fault type demonstrate that there are separate flow paths. For example, the Angel-type fault intersected at site 35-B carries a higher proportion of recent meteoric water than at 23-B. Boreholes intersecting the Pud fault produce a significant component of glacial meltwater. This is consistent with its lower permeability and orientation normal to the major principal stresses.

The depths currently reached by modern meteoric water are clearly due to the very high hydraulic gradients generated by creation of depressurized zones at

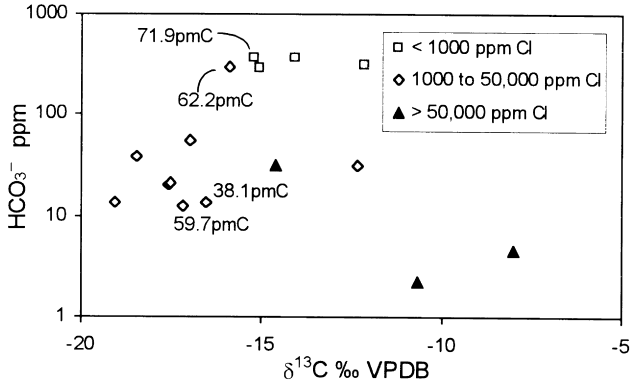

Fig. 6. Relationship between HCO_3^- and $\delta^{13}C_{DIC}$ in groundwater. Carbon-14 activities given for four samples analysed by AMS.

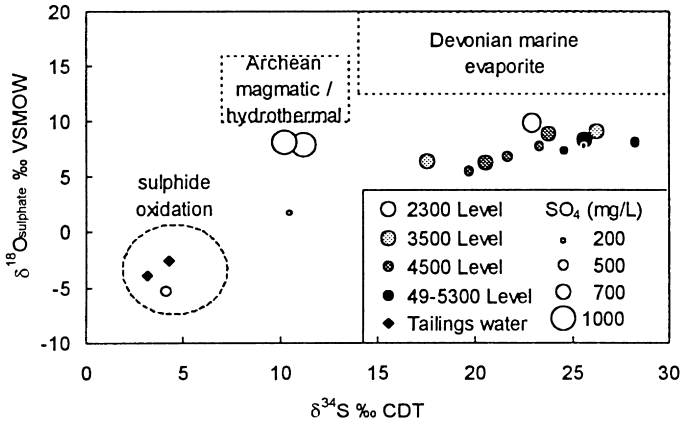

Fig. 7. $\delta^{18}O$ and $\delta^{34}S$ values for dissolved sulphate in groundwaters compared with possible sulphate sources. Approximate sulphate concentration given by size of data marker.

depth within the groundwater flow system by mine excavation. Monitoring since 1980 shows that this component has been increasing over time. Within a few months of drilling in 1979, flow from site 45-B comprised almost 60% glacial meltwater, but dropped to 20% by 1996 (Table 3, Fig. 5).

3.5. Mixing and geochemical evolution

Non-conservative geochemical species complement Cl^- and $\delta^{18}O$ water in tracing the circulation and mixing of the three groundwater components. In particular, the carbonate and sulphate systems provide insights into the recharge origin of waters and mixing dynamics.

The shallow, dominantly modern groundwaters have HCO_3^- up to 400 ppm with depleted $\delta^{13}C$ values (-14 to -17‰; Fig. 6) and attenuated ^{14}C activities. This is consistent with incorporation of soil derived CO_2 (estimated $\delta^{13}C \sim -23$ to -25‰, Clark and Fritz, 1997) during recharge followed by dissolution of hydrothermal calcite in the subsurface ($\delta^{13}C \sim -3 \pm 0.8$‰, $n = 5$).

In the brine samples, HCO_3^- concentrations are less than 10 ppm, and generally more enriched in ^{13}C (Fig. 6) due to exchange with hydrothermal calcite. Groundwaters with intermediate salinity (1–50 g/l Cl^-) show a depletion in ^{13}C. This is accounted for by a Rayleigh distillation in a closed system during mixing of high HCO_3^- groundwaters infiltrating from surface with high Ca^{2+} groundwaters at greater depths, forcing precipitation of calcite and decreasing bicarbonate concentrations. Most groundwaters are near or above saturation with respect to calcite, which has been observed as euhedral crystals in fractures. Sources of Ca^{2+} include mixing with the Ca^{2+}–Cl^- brines and dissolution of gypsum.

Gypsum dissolution in the shallow subsurface is suggested by the high SO_4^{2-} concentrations, which exceed 500–1000 ppm, and gypsum solubility indices, which approach saturation (Table 2). Values show a wide range of $\delta^{34}S$ from 3.1‰ to 28.3‰, and $\delta^{18}O$ from -5.4‰ to 9.7‰ (Fig. 7; Table 3). Potential sources of the sulphate include: (1) oxidation of pyrite; (2) Devonian marine evaporite; (3) magmatic/hydrothermal; and (4) sulphate from brines.

Depleted ^{34}S and ^{18}O contents characterize sulphate derived from oxidation of pyrite. This is the case for sample from tailings pond water (Fig. 7), which are within the range for pyrite from the mine reported by Wanless et al. (1960) (0.4–6.9‰). During sulphide oxidation, low $\delta^{18}O$ values can be anticipated due to the contribution of meteoric water (van Everdingen et al., 1985). Only one groundwater sample (23-E from the Negus Fault) has sulphate originating from the oxidation of pyrite. Sulphate in samples from the south end of all drifts are strongly enriched in $\delta^{34}S$, indicating no influence of mining activities on the chemistry of these groundwaters.

The deepest mine inflows are gypsum-saturated brines with SO_4^{2-} up to ~700 ppm and enriched isotope values ($\delta^{34}S \approx 25$‰, $\delta^{18}O \approx 8$‰), although

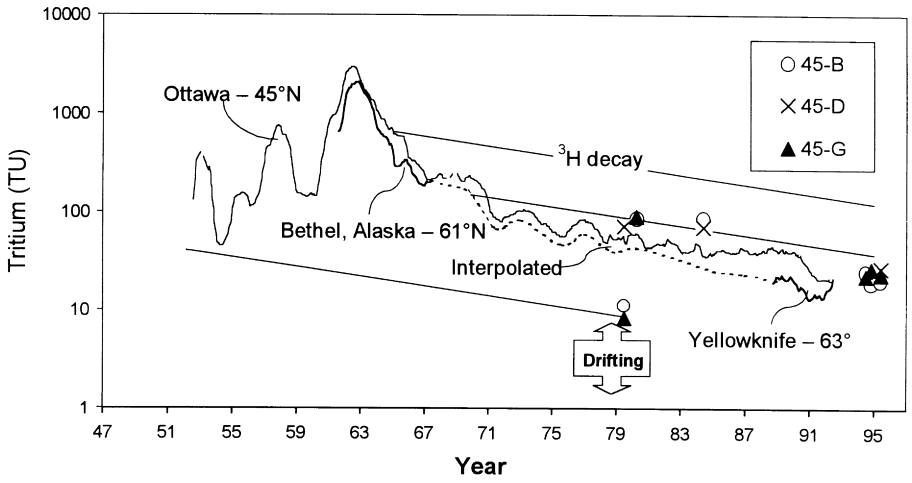

Fig. 8. The tritium input function used to model mean transit time (MTT) of groundwater inflows in mine was a combination of the limited data sets from from Bethel Alaska (1953–1968) and Yellowknife (1989–1993). The data were interpolated between 1968 and 1989 based on the ^{3}H record from Ottawa but with an attenuation factor of 0.7, which allowed a match with the Bethel and Yellowknife data. Tritium concentrations for samples on 4500 level, corrected for dilution with glacial and brine groundwaters (see text for discussion), are also given. Arrow indicates when drift construction took place on this level. Tritium decay lines are shown for example initial values. Precipitation data from IAEA Global Network for Isotopes in Precipitation (www.iaea.or.at:80/programs/re/gnif/gnipmain.htm).

Fritz et al. (1994) report $\delta^{18}O_{SO_4}$ values up to 16.7‰. This may indicate an origin as evaporated Paleozoic seawater, which has been proposed by Bottomley et al. (1999) on the basis of ^{6}Li and geochemical data. Published data for Devonian and Ordovician gypsum from near Gypsum Point, southwest of Yellowknife show δ^{34}S values of 15.1 and 22.6‰ (Claypool et al., 1980). Fritz et al. (1994) have suggested that the sulphate in these brines may have been introduced as a marine sulphate in the past and re-equilibrated with the brine water at temperatures of about 100°C, thus shifting the δ^{18}O values to the lower values observed now. Hattori and Cameron (1986) observed that δ^{34}S in sulphate of magmatic/hydrothermal origin in Archean greenstones is mostly in the range 8 to 14‰, which may account for the more ^{34}S-depleted samples collected from 2300 Level.

Most low salinity groundwaters from the upper levels have high sulphate concentrations with isotope values similar to those of the deep brines ($\delta^{18}O = 5.4$ to 9.7‰ and $\delta^{34}S = 19.7$ to 28.3‰). Thus, they cannot be derived by mixing with sulphate in the brines, but could originate as gypsum precipitated from the brines, possibly at the time of deglaciation. The pressure release on groundwater during deglaciation in the Yellowknife region would have approached 400 bar. Langmuir (1997) shows that the solubility constants of various sulphate minerals increase by about 40% for a 200 bar increase in pressure. The brines on 5300 Level are currently oversaturated with gypsum, while shallow groundwaters are near saturation with gypsum (Table 2). Further, sulphate minerals have been reported in the Con Mine subsurface (Hattori and Cameron, 1986). Prior to post-glacial flushing by infiltrating glacial meltwater and meteoric waters, brines likely occupied faults in the shallow subsuface and precipitated gypsum in faults and fractures upon depressurization during deglaciation.

3.6. Modelling rates of modern groundwater circulation with ^{3}H

Tritium (^{3}H) was used to calculate the mean transit time (MTT) of the modern groundwater component in mine inflows. It's short half-life (12.43 years) and high concentrations in precipitation from the atmospheric testing of thermonuclear devices since 1952, make it an important tracer for modern ($< \sim 50$ years) recharge. Tritium was measured at all underground sites sampled (Table 3) with the exception of 23-D, demonstrating that modern meteoric waters had

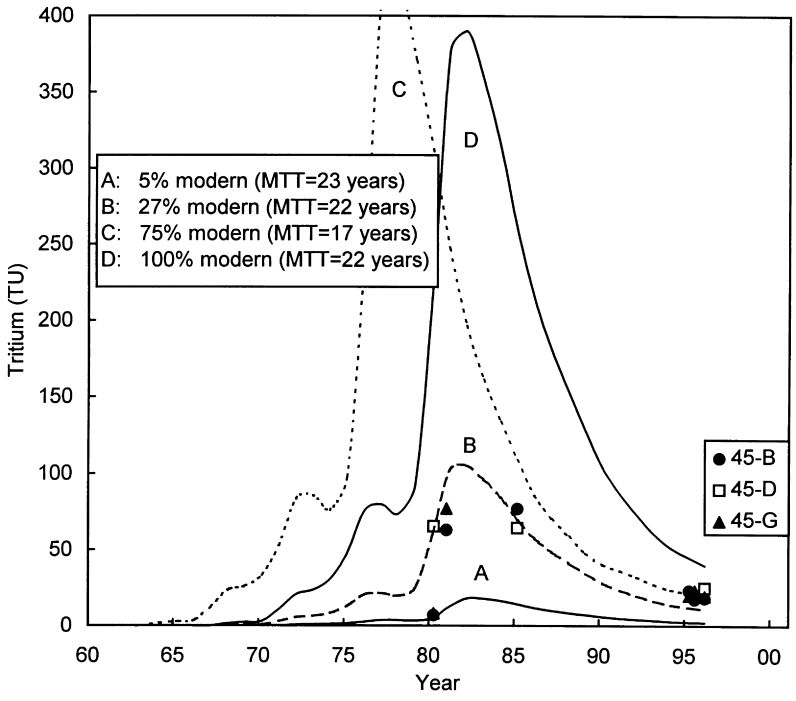

Fig. 9. Results for modelling mean transit times for recently recharged meteoric water sampled since 1980 at 45-B, using FLOW (Maloszewski and Zuber, 1996). Measured tritium concentrations, corrected for dilution by tritium-free brine and glacial meltwater, are compared with best-fit models for mean transit times (MTT). Models specify mixing of modern (tritiated) and sub-modern (tritium-free) meteoric waters.

infiltrated to all levels sampled in the study area. The absence of detectable tritium 38 years after the 23-D site was drilled is consistent with its low flow rate from a low permeability fracture. This hole intersected none of the three main faults, and has a discharge of only 0.01 l/min. By contrast, the other boreholes all intersected one or more of the principal faults, and had significantly greater flow and tritium (up to 57 TU). The lowest ^{3}H contents are observed for the deepest sites at 1615 m below surface (5300 level) where only a very minor component of modern meteoric water has mixed with the brine and glacial water.

Repeated sampling of inflows on the 4500 level since 1980 has allowed calculation of surface-to-depth transit of the modern meteoric component. Tritium data from 1980 to 1996 for sites 45-B, 45-D and 45-G on the 4500 level are plotted in Fig. 8. These data have been corrected for dilution with brine and glacial meltwater components to give the concentration in 100% meteoric water, using the mixing calculations presented above. For example, the value of 3 TU measured at site 45-B in 1980 is corrected to 10.7 TU, based on this sample having only 28% modern water. Thus, we are modelling the MTT of the modern meteoric water component, and not the glacial or brine components. The error in the corrected ^{3}H value generated by a 2‰ uncertainty in the $\delta^{18}O$ value assigned to the mixing end-members, discussed above, is minor: 10.7 ± 3 TU for the early data (July 1980), and 88.4 ± 6 TU for the high ^{3}H data (June 1985).

The corrected tritium content was then used to model MTT of the modern meteoric water component using a combined exponential flow–piston flow model (FLOW, Maloszewski and Zuber, 1982, 1996). The input data set for ^{3}H in precipitation included monitoring data from Yellowknife (63°N; 1989–1993) and Bethel, Alaska (61°N; 1962–1968) with interpolation between 1969 and 1988 based on monitoring data from Ottawa (45°N) attenuated to match the Yellowknife and Bethel data (Fig. 8).

Mean annual rather than mean monthly values were used, as we have no data to demonstrate any seasonal bias in recharge. The model allows that the sampled water comprises a modern (post-thermonuclear testing) component mixed with a sub-modern, tritium-free component. Optimum matches with the corrected tritium data for 4500 level groundwater were obtained where the modeled effect of piston flow (non-dispersive flow) was four times greater than that of exponential flow (multi-year contributions to recharge).

Modelling results are shown in Fig. 9. Assuming no dilution with ^{3}H-free water, curve D was the best overall match to the data, although it greatly overestimated the tritium content. This demonstrates that there is dilution by a sub-modern (but not glacial), tritium-free component, such as that seen at site 23-D. This component has the same geochemical and isotopic characteristics of the modern (tritiated) water, but would have been recharged prior to 1952. Curves A, B and C represent the best matches to the data, using a range of modern/sub-modern mixtures. With references to changes in water composition observed since 1980 at 45-B (Fig. 5), it is reasonable to assume that sub-modern meteoric water has been flushed by modern recharge during the period of mining in the same way as was the glacial meltwater. This accounts for the very high modern water dilution required to match the 1980 data (curve A) and the lower dilutions indicated for the later data (curves B and C).

Results indicate a 23-year MTT for 1980–1985 inflows on the 4500 level, decreasing to 17 years for inflows during 1995–1996. The longer initial transit times may relate to the time period required for depressurization to propagate upward and towards a steady state condition. Thus, the recent meteoric water component discharging at this level in 1980 (only one year after drifting) and 1981 was recharged prior to the main period of thermonuclear bomb testing (1958–1963). The best fit to the most recent data (1995–1996) indicates that the recent meteoric water fraction discharging on the 4500 level was recharged about 1980.

4. Conclusions

Groundwater inflows sampled from drifts excavated into the southern, unmined area of the Con Mine, are mixtures of Shield brine, glacial meltwater and recent meteoric recharge. The Ca^{2+}–Cl^{-} brines, with Cl^{-} up to 185 g/l, are ubiquitous in the Canadian Shield setting, and dominate at this site at depths of 1372 m, and greater. Shallow groundwaters are dominated by modern meteoric water. They have gypsum saturation indices close to 1 and sulphate isotopic values are similar to those in the brine, suggesting that the brines once occupied a shallow level in mine faults. Circulation of glacial meltwaters at the end of the Pleistocene then flushed these brines from faults to depths as great as 1600 m.

Mining activities, beginning in 1937, induced deep circulation of meteoric waters, identified as both sub-modern (pre-thermonuclear era) and modern (tritiated) groundwater. Today, modern, ^{3}H-bearing, meteoric waters follow strong vertical hydraulic gradients to all sample depths in the mine. The most permeable faults, oriented sub-parallel to the major principal stess direction, have the highest components of recent meteoric water. At the onset of sampling in 1980, the glacial meltwater contribution to inflows at 1370 m depth was up to 60% and has decreased to 20% as the proportion of modern meteoric water increased from less than 30% to over 70%.

Tritium measurements show that breakthrough of modern groundwaters at 1370 m depth occurred within about a year of drifting on this level. Exponential–plug flow modelling of tritium data suggests that MTT to the 4500 level were in the order of 20–25 years following excavation to this depth in 1979, an decreased to about 15–20 years by 1995. Further, the proportion of a tritium-free component of the recent meteoric water (i.e. $> \sim 50$ years old) has also decreased over the past two decades.

As an analogue for a radioactive waste repository, we conclude two principal points. Where permeable faults and fractures exist, underground openings at depth rapidly generate steep hydrodynamic gradients, allowing groundwater to circulate to depth with MTT of the order of two decades. Secondly, under conditions of low hydraulic gradients, deep groundwater circulation in highly permeable faults is minimal. At this site, glacial melt waters recharged at ca 10 ka remained in the subsurface up to the onset of mining activities. In the case of a radioactive waste repository, this

suggests that if the steep hydraulic gradients imposed during excavation and operation decay to natural conditions following closure, the potential for advective transport from depth to surface would be greatly diminished.

Acknowledgements

The geologists and staff at the Mirimar Con Mine are thanked for providing access and logistical support for underground and surface sampling at the mine. Wendy Abdi, Gilles St. Jean and John Loop are thanked for their assistance with isotropic and geochemical analyses. This work was funded by the Atomic Energy Control Board of Canada.

References

Bottomley, D.J., Gascoyne, M., Kamineni, D.C., 1990. The geochemistry, age and origin of groundwater in a mafic pluton, East Bull Lake, Ontario, Canada. Geochimica et Cosmochimica Acta 54, 993–1008.

Bottomley, D.J., Gregoire, D.C., Raven, K.G., 1994. Saline groundwaters and brines in the Canadian Shield: Geochemical and isotropic evidence for a residual evaporite brine component. Geochimica et Cosmochimica Acta 58 (5), 1483–1498.

Bottomley, D.J., Katz, A., Chan, L.H., Starinsky, A., Douglas, M., Clark, I.D., Raven, K., 1999. The origin and evolution of Canadian Shield brines: evaporation or freezing of seawater. Chemical Geology 155, 295–320.

Campbell, N., 1948. West Bay Fault. In: Structural geology of Canadian ore deposits. Canadian Institute of Mining and Metallurgy Jubilee Volume. 1948, pp. 244–259.

Clark, I.D., Fritz, P., 1997. Environmental Isotopes in Groundwater, Lewis, Boca Raton, FL (pp. 328).

Clark, I.D., Douglas, M., Raven, K., Bottomley, D., 2000. Infiltration and preservation of Laurentide Ice Sheet meltwater in the Canadian Shield. Ground Water (in press).

Claypool, G.E., Holser, W.T., Kaplan, I.R., Sakai, H., Zak, I., 1980. The age curves of sulphur and oxygen isotopes in marine sulphate and their mutal interpretation. Chemical Geology 28, 199–260.

Craig, B.G., 1965. Glacial Lake McConnell, and the surficial geology of parts of Slave River and Redstone River map-areas, District of Mackenzie; Geological Survey of Canada, Bulletin 122, 33pp.

Cwynar, L.C., Ritchie, J.C., 1980. Arctic-steppe tundra: a Yukon perspective. Science 208, 1375–1377.

Dansgaard, W., Clausen, H.B., Gundestrup, N., Hammer, C.U., Johnsen, S.J., Kristinsdottir, P.M., Reeh, N., 1982. A new Greenland deep ice core. Science 218, 1273–1277.

Dyke, A.S., Dredge, L.A., 1989. Quaternary geology of the northwestern Canadian Shield. In Chapter 3 of Quaternary Geology of Canada and Greenland, Fulton, R.J. (ed.); Geological Survey of Canada, Geology of Canada, no. 1 (also Geological Society of America, The Geology of North America, v. K-1).

Frape, S.K., Fritz, P., 1982. The chemistry and isotopic composition of saline groundwaters from the Sudbury basin, Ontario. Canadian Journal of Earth Sciences 19, 645–661.

Frape, S.K., Fritz, P., McNutt, R.H., 1984. Water–rock interaction and chemistry of groundwaters from the Canadian Shield. Geochimica et Cosmochimica Acta 48, 1617–1627.

Fritz, P., Reardon, E.J., 1979. Isotopic and chemical characteristics of mine water in the Sudbury area. AECL Technical Report 35, Atomic Energy of Canada Limited, Chalk River, Ontario, Canada, 37p.

Fritz, P., Frape, S.K., Drimmie, R.J., Appleyard, E.C., Hattori, K., 1994. Sulphate in brines in the crystalline rocks of the Canadian Shield. Geochimica et Cosmochimica Acta 58, 57–65.

Gascoyne, M., Kamineni, D.C., 1994. The hydrogeochemistry of fractured plutonic rocks in the Canadian shield. Applied Hydrogeology 2, 43–49.

Hattori, K., Cameron, E.M., 1986. Archean magmatic sulphate. Nature 319 (6048), 45–47.

Henderson, J.F., Brown, I.C., 1966. Geology and structure of the Yellowknife Greenstone Belt, District of Mackenzie. Geological Survey of Canada, Bulletin 141, 87pp.

Hillaire-Marcel, C., Soucy, J.-M., Cailleux, A., 1979. Analyse isotopique de concrétions sous-glaciaires de l'inlandsis laurentidien et teneur en oxygène 18 de la glace. Canadian Journal of Earth Sciences 16, 1494–1498.

Intera Consultants Ltd., 1997. Hydrogeological and hydrogeochemical study of the Miramar Con Mine, Yellowknife, NWT. Report prepared for the Atomic Energy Control Board of Canada.

Kharaka, Y.K., Gunter, W.D., Aggarwall, P.K., Perkins, E.H., De Braal, J.D., SOLMINQ88: a computer program code for geochemical modelling of water–rock interactions. US Geological Survey Water Investigations, Report 88, 1988.

Koerner, R., Fisher, D.A., 1990. A record of Holocene summer climate from a Canadian high Arctic ice core. Nature 343, 630–631.

Langmuir, D., 1997. Aqueous Environmental Geochemistry, Prentice-Hall, New Jersey.

Lindberg, P.A., 1987. An investigation of the Pud and Negus Fault offsets of the Campbell Shear Zone, Con Mine, Yellowknife, Northwest Territories, Report prepared for Nerco Minerals Company.

Macdonald, I.M., 1986. Water–rock interaction in felsic rocks of the Canadian Shield. MSc thesis, Waterloo University.

Maloszewski, P., Zuber, A., 1982. Determining turnover time of groundwater systems with the aid of environmental tracers. I. Models and their applicability. Journal of Hydrology 57, 207–231.

Maloszewski, P., Zuber, A., 1996. Lumped parameter models for interpretation of environmental tracer data (Supplementary Annex). In: Manual on Mathematical Models in Isotope Hydrogeology. IAEA-TECHDOC-210, IAEA, Vienna.

McDonald, D.W., Duke, N.A., Hauser, R.L., 1993. Geological setting of the NERCO Con Mine and the relationship of gold

mineralisation to metamorphism, Yellowknife, N.W.T. Exploration Mining Geology 2 (2), 139–154.

Moorman, B.J., Michel, F.A., Drimmie, R.J., 1996. Isotope variability in Arctic precipitation as a climatic indicator. Geoscience Canada 23, 189–194.

Pearson, F.J., Jr., 1987. Models of mineral controls on the composition of saline groundwaters in the Canadian Shield. In: Fritz, P., Frape, S.K. (Eds.), Saline waters and gases in crystalline rocks. Geological Association of Canada Special Paper 33, pp. 39–51.

Sofer, Z., Gat, J.R., 1972. Activities and concentrations of oxygen-18 in concentrated aqueous salt solutions: analytical and geophysical implications. Earth Planetary Science Letters 15, 232–238.

van Everdingen, R.O., Shaku, M.A., Michel, F.A., 1985. Oxygen- and sulfur-isotope geochemistry of acidic groundwater discharge in British Columbia, Yukon, and District of Mackenzie, Canada. Canadian Journal of Earth Sciences 22, 1689–1695.

Wanless, R.K., Boyle, R.W., Lowden, J.A., 1960. Sulphur isotope investigation of the gold-quartz deposits of the Yellowknife district. Economic Geology 55, 1591–1621.